Volume Graphics (2005)
E. Gröller, I. Fujishiro (Editors)

Scaffolding-based Segmentation of Coronary Vascular Structures

Dirk Bartz[1†] Sarang Lakare[2‡]

[1]Visual Computing for Medicine, University of Tübingen
[2]Center for Visual Computing, Stony Brook University

Abstract

The coronary arteries are essential for the proper function of the human heart. However, they are generally difficult to segment in volume datasets separately from the other blood-filled cavities of the heart. The major reason for these difficulties is the lack of sufficient spatial resolution and partial volume effects.
In this paper, we present a method to mark the coronary arteries by a virtual endoscopic traversal. Virtual endoscopy enables a significantly easier visual identification of the blood vessels in comparison to outside views or slice-by-slice examination methods. Furthermore, we use this marking as a scaffold for the actual segmentation of the coronary arteries.
Keywords: *Virtual Medicine, Cardio-Vascular System, Segmentation, Virtual Endoscopy*

Categories and Subject Descriptors (according to ACM CCS): I.3.7 [Three-Dimensional Graphics and Realism]: Virtual Reality I.3.8 [Application]: Virtual Medicine J.3 [Life and Medical Sciences]: Cardiology, Radiology

1. Introduction

The vascular system is one of the most important and challenging organ systems in the human body. It ensures circulation and distribution of oxygen, nutrients, hormones, and cells of the immune defense system through all parts of the body. While doing so, it regulates fundamental physiological measures, such as body temperature, hormonal and acid-base balance.

The centerpiece of the vascular system is the heart, which pumps blood through the vascular system. Any disturbance of this system can have a significant impact on body functions. In particular disorders of coronary blood vessels – which supply the heart muscle – can lead to destructions of the respective muscle areas. The resulting malfunction of the heart muscle can cause severe disturbances of the heart rate, which influences the ejection rate of the heart, in particular of the left ventricle (see Section 2).

For the timely diagnosis of pathologies of coronary blood vessels, cardio-vascular imaging is, next to other diagnostic means, essential. Unfortunately, imaging of the heart is an extremely challenging task. The frequency of the heartbeat varies usually between 60 and 80 beats per minute, while this number can be higher or lower, depending on body activity. This is too fast for all regular medical imaging modalities to avoid motion artifacts. Thus, scanning is usually triggered by the peak of the ECG, which measures the electric activity of the heart [FO01]. Currently, multi-slice CT scanners, which acquires parts of four to sixteen spirals at a time [KRSF*99, FO01], are considered state-of-the-art. Synchronized by the ECG, it scans only in specific parts of the heartbeat cycle to minimize motion artifacts.

The blood-filled cavities in the heart are enhanced by an injected contrast agent. However, effects like beam hardening [Ame05], due to high contrast agent density, can reduce the quality of data significantly. Fortunately, this effect is usually limited to the right atrium of the heart, which is less important for the assessment of coronary arteries. Of more concern is the fact that coronary blood vessels are extremely difficult to segment due to the limited spatial resolution of

† e-mail: bartz@gris.uni-tuebingen.de
‡ e-mail: lsarang@cs.sunysb.edu, currently with Siemens Medical Solutions

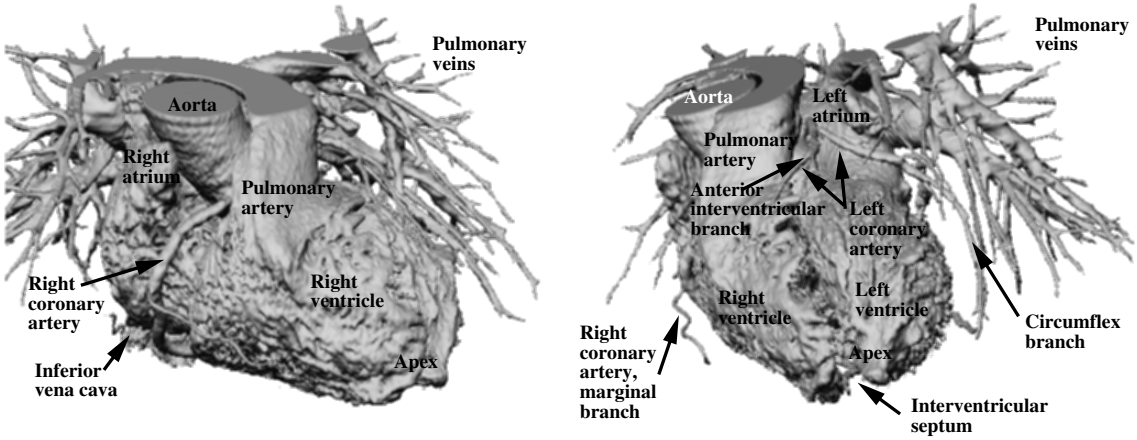

Figure 1: *Reconstructed blood-filled cavities of the heart; (a) anterior (front) view, (b) sinister (left) view.*

the scan. In this paper, we propose a marking method to accentuate coronary blood vessels in visualizations of the heart. We use this marked region to generate a segmentation of the coronary arteries. The marking itself is based on the virtual endoscopic exploration of coronary blood vessels.

In the course of this paper, we provide a short overview of the structure and function of the heart to understand the causalities that can lead from a stenosis to a failure of the heart function (Section 2). In Section 3, we review related work and present our approach for the representation and visualization of coronary blood vessels, and the respective results in Section 4. Finally, we conclude in Section 5.

2. Structure and Function of the Heart

The human heart is divided into four chambers; the left and right atrium and the left and right ventricles, whereas the left and right side of the heart are not directly connected with each other [HR85]. The right part of the heart (see also Fig. 1a) – right atrium and right ventricle – are connected through the atrioventricular valve (or tricuspid valve). The atrium receives the venous blood through the venae cavae from the body, whereas the ventricle pumps that blood through the pulmonary valve and through the pulmonary artery to the lungs. After the blood is enriched with oxygen in the lungs, it is received through the pulmonary veins in the left atrium, which is connected through the left atrioventricular valve (or mitral valve) with the left ventricle (see Fig. 1b). The ventricle pumps the enriched blood through the aortic valve into the aorta, which distributes the blood to the other body arteries. The (left and right) coronary arteries branch from the aorta and supply the heart muscle with enriched blood through a system of blood vessels that branch from the coronary arteries. They are complemented by the cardiac veins, which collect the blood and merge into a large vein (coronary sinus) that leads to the right atrium.

The conducting system of the heart consists of the sinuatrial node (which generates the electric trigger of the heartbeat), the atrioventricular node (AV node), the AV bundle, which distributes the conduction of the impulse to the ventricles, and at the end, the Purkinje fibers. Due to this arrangement, the contraction of the heart starts at the apex and moves quickly towards the aorta and pulmonary artery, and thus pumps the blood from the ventricles to the respective arteries. A more detailed description of the heart can be found in anatomy text books [HR85].

Cardiac problems often arise from a stenosis of a coronary artery, which is a stricture of this blood vessel that limits the possible blood flow through that part of the vessel and – depending on its severeness – can cause serious cardiac problems, up to an *angina pectoris*, a temporary insufficient supply of oxygen to the heart muscle. Over time, it might even develop into an occlusion of the respective coronary arteries, which causes a serious disturbance of the coronary blood flow. The resulting dysfunctional parts of the respective heart muscle jeopardize the synchronized contraction of the heart, lead to a completely uncoordinated partial contraction, and henceforth reduce the pumping performance of the heart dramatically. This is one of the major causes of heart failure. Other possible causes of cardiac problems are direct damages to the conducting system, which jeopardize the electrical function of the heart, or malfunctions of the numerous valves in the blood flow controlling heart.

3. Related Work

The heart is of central interest in the medical community. Consequently, a large number of related publications are

available, which focuses on the various aspects from assessment, diagnosis, treatment, imaging, and modeling. In this section, we can only give a brief overview of aspects that vary from imaging of relevant features to the assessment of the function of the cardio-vascular system, which might be supported by computer graphics methods. These aspects furthermore range from methods with direct clinical application to methods that are still a research topic.

Echo-Cardiography (or Doppler Myocardial Imaging) is a non-invasive ultrasound based technique that is used for the evaluation of the speed of the blood flow, i.e. the blood flow through the valves of the heart, and other assessments [WDGM01]. With the invasive intra-vascular ultrasound imaging, a probe is introduced into the blood vessels of interest [WMR*01]. Other methods include MRI Angiography (MRA) or MRI perfusion imaging to assess the blood flow. The blood flow itself can be simulated by CFD methods, based on the derived geometry of the heart [FKL*00]. Fenlon et al. described a system that simulates flexible artificial heart valves to evaluate the performance of the various designs [FDW00].

Another direction of research aims at the modeling of the mechanical, electrical, and cell-based functions of the heart, which often is in the domain of biomedical engineering. Park et al. [PMA*99] studied the motion (contraction) of the ventricles of the heart to assess the function and Montillo et al. focused on the segmentation of the left and right ventricles [MMA02]. Sachse et al. investigate the electro-mechanical properties of the left ventricles [SSW02] and McCulloch et al. looked into these properties from cellular level up to organ level [MBHN98]. Most of the research done in modeling of the heart is based on the extensive analysis of image data. Sachse et al. for example used a segmentation of the visible male [SSW02]. Virtually all methods that include modeling have in common that up to now, an application to patient data is technically possible, but not practical, in particular for an application in a clinical routine setting.

Essential for a patient oriented presentation of blood vessels are appropriate segmentation methods. Numerous techniques are available for various kinds of blood vessels. Young et al. presented next to their own, shape-based propagation blood vessel extraction algorithm an overview of other approaches [YPW01]. However, almost all of these approaches are targeting blood vessels in areas like the head [BAL*99], the lungs [BMF*03], the liver [SPSP02], the neck, or the extremities [KWF*01], where frequently a graph representation of the vessel tree based on its skeleton is generated [BAL*99, SPSP02]. La Cruz et al. presented a model-based parameterization model for the reconstruction blood vessels [CSK*04]. Unfortunately, coronary blood vessels pose a significantly different challenge, due to the signal similarities of the blood (and contrast agent) filled heart and blood vessels. Hence, many of the presented methods cannot differentiate adequately between cavities of the heart and the coronary blood vessels. They are therefore not suited for coronary blood vessels.

Recent methods however, have been successfully applied to the coronary blood vessels of the heart. Lorenz et al. proposed a three level segmentation method of the coronary blood vessels using fast-marching wave front propagation [LRSB03]. The three levels (voxels, segments, tree) trim the segmentation to represent the coronary blood vessel tree. This segmentation information can be combined to generate a 3D graph representation of the vessel tree, like it has been done for cerebral blood vessels [BAL*99]. In contrast, we are aiming at situations, where (semi-)automatic methods fail to reconstruct coronary blood vessels, due to various artifacts. Sherbondy et al. presented an approach that also employs interaction to improve the segmentation result [SHN03]. They visualize the segmentation result and control similar to the approach presented here segmentation leaks with a mask based on the segmentation seeds.

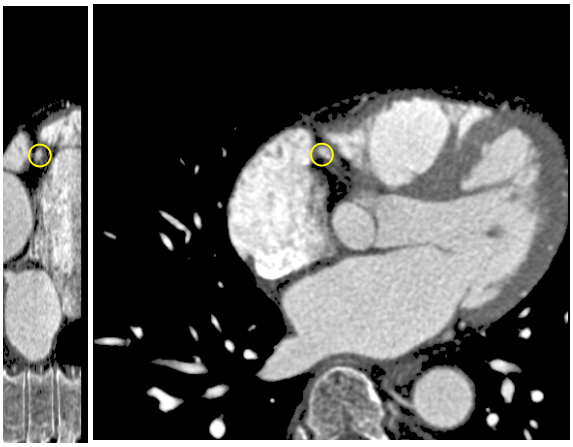

Figure 2: *Slice views of heart dataset. Sagittal (left) and axial slice (pre-segmented) (right) with coronary arteries - the current position (within the* right coronary artery*) is marked with the circle.*

The volume data for the patient oriented visualization of the relevant features of the heart is acquired by helical CT scanners that are synchronized with an ECG. With the introduction of multi-slice CT scanners, a higher spatial resolution became available that enables better reconstructions of anatomical features [KRSF*99, FO01]. These patient datasets can be used for advanced visualization of features of the coronary arteries. In 2001, we used virtual endoscopy to explore features such as stenosis of coronary arteries [BGL*01] (see also Fig. 4). Schroeder et al. [SKO*02] presented a study where virtual endoscopy (virtual coronary angioscopy) was used to detect lesions of the coronary arteries. In contrast, we use virtual endoscopy here to mark the visited coronary blood vessels for further post-processing.

Please note that although we examined only CT data, the

presented methods are not limited to this kind of data and could be used for all other types of volume data of the cardiovascular system (if the anisotropy is adequately addressed). However, CT scanners are the current state-of-the-art in analyzing the morphology of the heart (our focus), while MRI scanners usually focus on functional aspects.

4. Reconstruction of Coronary Blood Vessels

In heart datasets, we can find several different kinds of blood vessels. Easy distinguishable – although still difficult to segment – are the large veins, the aorta, and the pulmonary artery and veins (see Fig. 1). Significantly smaller, and hence more difficult to identify is the complex system of coronary blood vessels. Whereas segments of them can be identified while taking a closer look at the data (see Fig. 1) or using specific blood vessel tracing algorithms [BFC02], it is challenging to locate the whole system of coronary arteries. Most of the problems are caused by partial volume effect artifacts and the lack of sufficient spatial resolution – the multi-slice CT scan (four slices) provides a slice distance of less than 1.3mm, and a pixel distance of about 0.5mm. While the latter one diminishes some of the boundaries between the ventricles of the heart and the coronary vessels (see circled area in Fig. 2), the partial volume effect leads to artificial connections or holes that are not present in the scanned subject. These connections or holes are resulting from averaging operations that compensate violations of the sampling theorem at volume reconstruction (undersampling) in regions with high intensity differences between neighboring voxels.

From an endovascular view (see Fig. 3 and 4) fractions of the affected blood vessels are still visible and usually provide sufficient hints on their shape, which cannot easily be spotted from an outside view. Therefore, the paths of these blood vessels are significantly easier to identify from an endovascular view (see Fig. 3). Therefore, we visit the coronary arteries starting from their common starting point in the aorta successively using our virtual endoscopy system [BS99].

4.1. Virtual Endoscopy

Our virtual endoscopy system VIVENDI [BS99] enables the virtual exploration of patient volume data from endoscopic viewpoints. First, the voxels of interest are segmented with standard threshold and 3D region-growing methods. Unfortunately, bone structures and contrast agent enhanced blood-filled cavities have approximately the same density values. In some cases, this requires additional cut-off operations to remove false connections. Furthermore, the complex tree-like structure of the pulmonary veins often obstructs the outside view on the coronary arteries. Since they are usually not in the focus of coronary imaging, we also cut-off these structures. In total, the standard segmentation takes about one minute. If additional cut-off operations are required, segmentation takes approximately five to 15 minutes.

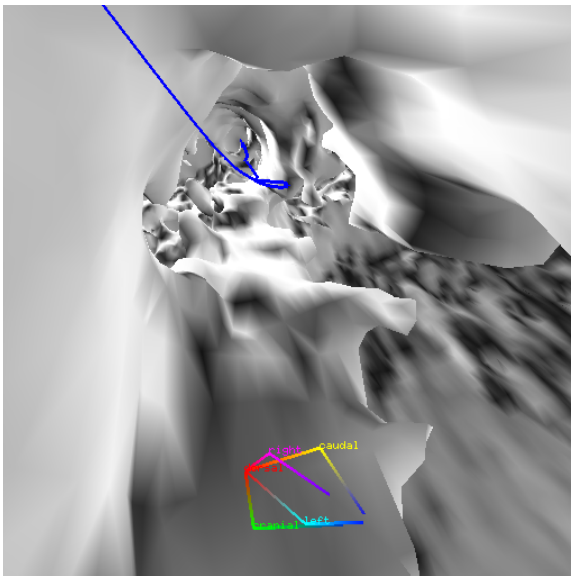

Figure 3: *Virtual endoscopic view through coronary arteries; the blue/black line is the marked path through the arteries. The reconstruction of the* circumflex branch *of the* left coronary artery *is incomplete due to the lack of spatial resolution and partial volume effects.*

Based on the segmentation, the inner surface of the cavities is reconstructed and represented by a polygonal mesh that is organized hierarchically by an octree decomposition of the volume dataset. Also based on the segmentation of the body cavities of interest, we generate a set of potential fields that implement a collision avoidance system[†] [BS99].

Note that this segmentation is extracting all of the blood-filled cavities of the heart, and is therefore not suited for the segmentation of the coronary blood vessels alone.

4.2. Virtual Coronary Angioscopy

We are using the described virtual endoscopy system to interactively visit the coronary blood vessels. Starting from the aorta – the coronary arteries branch from the aorta –, we successively traverse the coronary arterial system. If the current blood vessel branches, we recursively visit any of its branches and return to the branching point, which was previously bookmarked manually through the scout module of VIVENDI [BS99]. In cases where the wall of the blood vessels could not be successfully reconstructed – lacking suf-

[†] The potential fields also implement user-guidance to a specified target area [BS99]. However, the semi-automatic exploration of the coronary arteries based on this user-guidance would require an already successful segmentation and is thus not practical in our scaffolding approach.

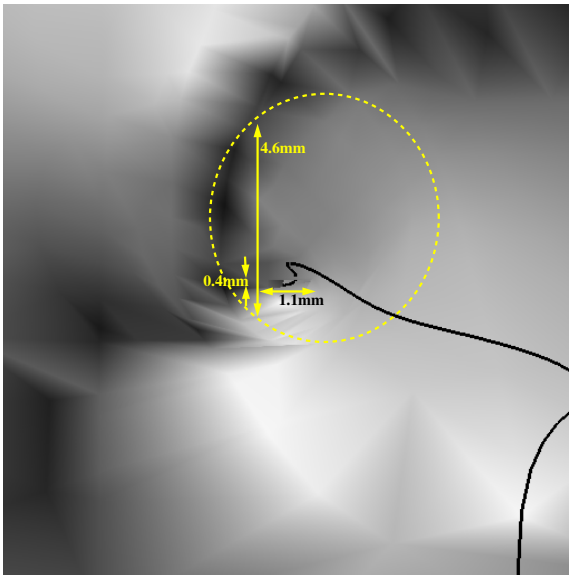

(b)

Figure 4: *Virtual endoscopic view through coronary arteries; the black line is the marked path through the arteries. The figure shows a stenosis of* left anterior descent (LAD) *and the progress of the stenosis compared to the regular vessel diameter (regular vessel shape marked with yellow circle).*

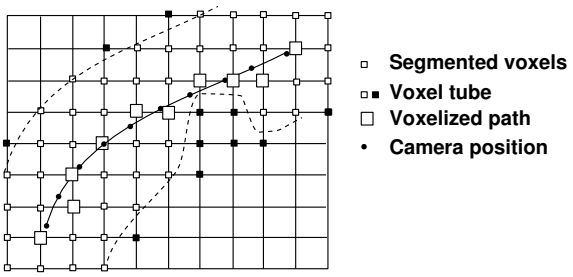

Figure 5: *Path voxelization and segmentation: The positions of the camera path (solid line) are used for the voxelized path in the blood vessel (dashed lines). Subsequently, a 26-neighborhood voxel tube is created around the voxelized path, representing the segmentation scaffold. A stenosis is located at the right part of the blood vessel and excludes voxels of the scaffold (black cubes) from the segmentation.*

ficient spatial resolution – tracing of the direction becomes more difficult (see Fig. 3). Although segmentation methods will usually not succeed segmenting this blood vessel, the direction and shape of it are still apparent from an endoscopic viewpoint (Fig. 3). Hence, we can continuously traverse the artery. In rare cases, the blood vessel data completely resolves into the neighboring chamber of the heart. Fortunately, such location rarely exhibits sudden changes of direction of that blood vessel, which in turn simplifies the task of finding the blood vessel, once it appears again.

At the time of our traversal, we mark the locations of our virtual camera, similar to Greek myth of the Minotaur, where Ariadne's thread leads out of its labyrinth. This marking can later be used to visualize the journey of the camera through the vascular system (see Fig. 7 and 8). Since the camera travels through the volume cells of the patient dataset, we can also generate a voxelized path. For this voxelization, we simply select the nearest-neighbor voxel to the current camera position. The smooth interpolation and the physically-based motion model of the virtual camera by the guided navigation system [BS99] ensures a continuous and smooth voxel path (see Fig. 3 and 4). However, if the step size of the camera is too large, we need to connect subsequent camera positions to generate a voxel path. This is achieved by attaching line segments between the positions to be connected. Since these line segments are always short (if needed at all), they still preserve a smooth appearance. Afterwards, we assign a voxel environment (or tube) to that path, which represents the scaffold for the later segmentation of the visited blood vessels (see Fig. 6b). Using inverse *onion peeling* [HKW*95], we add n layers of voxels around the voxel path[‡]. n should reflect the typical voxel radius of the coronary blood vessels, possibly considering the rare case of aneurysms. Note that a large n may also include too many voxels into the scaffold that do belong to neighbor blood-filled cavities of the heart.

A distance field based voxel tube generation [ST94] would ensure a smoother appearance at higher computational costs. Since this is not really required, we opted for the simpler *onion peeling*. Figure 5 gives an overview of the path voxelization and segmentation scaffold.

Based on the generated segmentation scaffold, we can apply simple 3D region growing segmentation, using the relevant thresholds to identify contrast agent filled blood vessels. The scaffold acts like a mask that limits the selection of voxels for the segmentation to the voxel tube represented by the scaffold (Fig. 5). A stenosis of these blood vessels – a major target feature for coronary imaging – is covered by the segmentation scaffold, but the threshold interval controlled segmentation process also restricts the selection to the voxels within the relevant threshold interval (see black scaffold voxels in Fig. 5)[§]. Overall, our algorithm selects all voxels along the voxel path of the structures visited by the virtual endoscopy system, limited by the segmentation scaffold and

[‡] Each voxel of the next layer is in a 26-neighborhood of the previous layer.

[§] Note that partial volume effects and limited resolution can create artificial connections between neighboring high-contrast areas. The scaffold only limits their influence – resulting in leaking of the segmentation –, it does not completely remove it.

the relevant intensity interval of the contrast agent enhanced blood vessels. However, the current approach does not compensate for anisotropic data spacing. Hence, the implicitly uniform expansion of the segmentation scaffold will not ensure an uniform rendering of the vessel segmentation (see Fig. 7). It will grow larger into slice direction, where the voxel spacing (slice distance) is larger than within one slice (pixel distance). Fortunately, this effect is not very apparent in multislice CT data, since the slice distance is only two times larger than the pixel distance (0.6mm vs. 1.2mm).

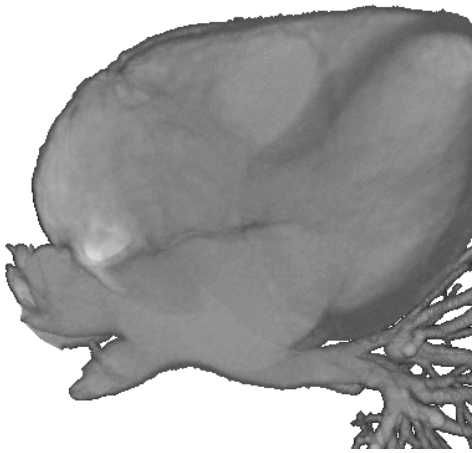

(a)

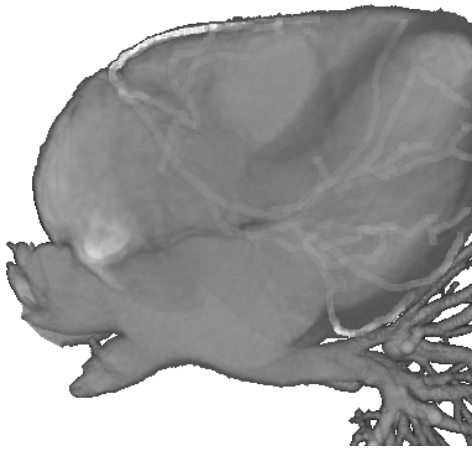

(b)

Figure 6: *Axial view of heart dataset; (a) pseudo x-ray image of heart data without marking, (b) pseudo x-ray image with voxel environment enhanced coronary arteries.*

Besides extracting the arterial vascular system of the heart, we can also segment the venous system. However, this system is usually less relevant for the diagnosis of coronary disorders.

4.3. Results

For the actual rendering, the segmented voxels are mapped into an isorange beyond the used isorange. For 8bit data, the scalar data range is downsampled to a smaller range (ie., $[0,240]$). The remaining value range of ($[241,255]$ in our example) is used for the segmentation, where the maximum value is assigned to the voxel path, whereas the voxel shells around the path has successively decreasing scalar values from $max-1$ (254) down to (max-n) (241 with $n=14$). If more than n voxel shells are required, the volume needs to be downsampled into a smaller data range, the voxel shells are assigned to a smaller range, or more bits per voxel are required. In our examples, the voxel shells fit into the specified range.

For high quality visualization of the coronary blood vessels, it is important to maintain the fuzzy boundary around the vessels where they interface with the surrounding objects. A loss of fuzzy boundary can lead to stair-casing artifacts in the rendered images. We extract the vessels with the intensity flipping technique [LK03] and then merge them with the original dataset. This allows us to visualize the smooth extracted blood vessels along with the heart.

The color plates of this paper (Fig. 7 and 8) demonstrate some of the rendering options with the enhanced coronary blood vessels. Figure 7a shows a volume rendered image (using the VIZARD II ray casting hardware [MKW*02]) of a heart dataset that is combined with the segmentation of the voxel environment of the marked coronary blood vessels. In Figure 7b, we see a close-up of the vessel tree of the left coronary artery, and the respective LAD stenosis. Figures 8a and b show images of the same heart, exposing a stenosis in the *left anterior descent* branch of the *left coronary artery*. The yellow lines show the camera paths of the virtual endoscopy traversals through this dataset (Fig. 8a). Figure 8b shows an overview of the zoom area of (a). Note that these camera paths are used to enhance the coronary blood vessels in Figure 7.

Figures 3 and 4 shows snapshots from virtual endoscopy. In the top image (a), we can see the incompletely reconstructed wall of the circumflex branch of the left coronary artery. Figure 4 shows a stenosis of left anterior descent (LAD) from an endoscopic viewpoint.

The total time requirements split into a data preprocessing part, which reconstructs the heart cavities and coronary blood vessels from the CT dataset, the interactive traversal of the coronary blood vessels, and finally the scaffolding-based segmentation. While data preprocessing accounts for approximately 5-15 minutes, depending on the acquisition quality of the dataset, the interactive traversal may take between 10 and 15 minutes depending on the experience of the user and the complexity of the dataset. The final scaffolding-based segmentation is only a matter of seconds.

Overall, this method is tremendously faster than manually

performing a slice-by-slice segmentation of the coronary arteries – in particular of small arteries –, but still too time consuming for clinical routine.

5. Conclusions and Future Work

In this paper, we presented a non-standard method for the segmentation of coronary blood vessels. Due to the limited spatial resolution, neighboring parts of the heart are commonly very difficult to separate from these coronary blood vessels. We use virtual endoscopy to traverse relevant blood vessels, thus marking them as blood vessels of interest. Based on the marking, we generate a scaffold for the segmentation of these vessels.

The major drawback of this method is the time consuming traversal of the blood vessels itself. Depending on the cardiac experience of the user and the quality of the volume data, it can take a significant amount time, which is usually not available in the daily clinical practice. However, it is still tremendously faster and easier to use – hence more practical – than the manual slice-by-slice segmentation used so far.

Future work will focus on a better representation of the segmentation. Currently, we simply specify the respective voxels and mask the volume dataset with the segmentation. However, a smoother representation can be generated, if we apply smooth voxelization methods, ie. the Vxt library [SK99]. With this approach, we can also adapt to the anisotropic nature of many datasets, in particular datasets from MRI and single-slice CT scanners.

Last but not least, this segmentation approach needs to be validated on phantom data and on a larger number of CT heart datasets.

Acknowledgments

The multi-slice CT datasets are courtesy of Siemens Medical Systems and the Department of Radiology of the University Hospital in Tübingen. We would like to thank Axel Küttner and Andreas Kopp of the Department of Radiology at the University Hospital in Tübingen and Stefan Schaller of Siemens Medical Solutions in Erlangen for providing datasets of the heart. We also would like to thank Özlem Gürvit at the Department of Radiology at the University Hospital in Marburg for helpful discussions, and Urs Kanus of the University of Tübingen for proof reading.

The work has been supported by the project CatTrain of the German Research Council (DFG), the Center of Competence for Minimally Invasive Medicine and Technology Tübingen-Tuttlingen (MITT), and the Department of Neurosurgery of the University of Tübingen.

References

[Ame05] AMERSHAM HEALTH: Medcyclopaedia - Encyclopaedia of Medical Imaging. http://www.amershamhealth.com/medcyclopaedia/medical/, accessed 2005. 1

[BAL*99] BULLITT E., AYLWARD S., LIU A., STONE J., MUKHERJI S., COFFEY C., GERIG G., PIZER S.: D Graph Description of the Intracerebral Vasculature from Segmented MRA and Tests of Accuracy by Comparison with X-ray Angiograms. In *Proc. of Information Processing in Medical Imaging, LNCS 1613* (1999), pp. 308–321. 3

[BFC02] BÜHLER K., FELKEL P., CRUZ A. L.: *Geometric Methods for Vessel Visualization and Quantification - A Survey*. Tech. Rep. 35, VRVis Wien, Austria, 2002. 4

[BGL*01] BARTZ D., GÜRVIT O., LANZENDÖRFER M., KOPP A., KÜTTNER A., STRASSER W.: Virtual Endoscopy for Cardio Vascular Exploration. In *Proc. of Computer Assisted Radiology and Surgery* (2001), pp. 960–964. 3

[BMF*03] BARTZ D., MAYER D., FISCHER J., LEY S., DEL RÍO A., THUST S., HEUSSEL C., KAUCZOR H., STRASSER W.: Hybrid Segmentation and Exploration of the Human Lungs. In *Proc. of IEEE Visualization* (2003), pp. 177–184. 3

[BS99] BARTZ D., SKALEJ M.: VIVENDI - A Virtual Ventricle Endoscopy System for Virtual Medicine. In *Proc. of Symposium on Visualization* (1999), pp. 155–166,324. 4, 5

[CSK*04] CRUZ A. L., STRAKA M., KOECHI A., SRAMEK M., GRÖLLER E., FLEISCHMANN D.: Nonlinear Model Fitting to Parameterize Diseased Blood Vessels. In *Proc. of IEEE Visualization* (2004), pp. 393–400. 3

[FDW00] FENLON A., DAVID T., WALTON J.: An Integrated Visualization and Design Toolkit for Flexible Prosthetic Heart Valves. In *Proc. of IEEE Visualization* (2000), pp. 453–456. 3

[FKL*00] FORSBERG A., KIRBY R., LAIDLAW D., KARNIADAKIS G., VAN DAM A., ELION J.: Immersive Virtual Reality for Visualizing Flow Through an Artery. In *Proc. of IEEE Visualization* (2000), pp. 456–460. 3

[FO01] FLOHR T., OHNESORGE B.: Heart Rate Adaptive Optimization of Spatial and Temporal Resolution for Electrocardiogram-Gated Multislice Spiral CT of the Heart. *Journal of Computer Assisted Tomography 25* (2001), 907–923. 1, 3

[HKW*95] HONG L., KAUFMAN A., WEI Y., VISWAMBHARAN A., WAX M., LIANG Z.: 3D Virtual Colonoscopy. In *Proc. of IEEE Symposium on Biomedical Visualization* (1995), pp. 26–32. 5

[HR85] HOLLINSHEAD W., ROSSE C.: *Textbook of Anatomy*, 4th ed. Harper & Row, Publishers, Philadelphia, USA, 1985. 2

[KRSF*99] KLINGENBECK-REGN K., SCHALLER S.,

FLOHR T., OHNESORGE B., KOPP A., BAUM U.: Subsecond Multi-slice Computed Tomography: Basics and Applications. *European Journal of Radiology 31*, 2 (1999), 110–124. 1, 3

[KWF*01] KANITSAR A., WEGENKITTL R., FELKEL P., FLEISCHMANN D., SANDNER D., GRÖLLER E.: Computed Tomography Angiography: A Case Study of Peripheral Vessel Investigation. In *Proc. of IEEE Visualization* (2001), pp. 477–480. 3

[LK03] LAKARE S., KAUFMAN A.: Anti-Aliased Volume Extraction. In *Proc. of Symposium on Visualization* (2003), pp. 113–122. 6

[LRSB03] LORENZ C., RENISCH S., SCHLATHÖLTER T., BÜLOW T.: Simultaneous Segmentation and Tree Reconstruction of the Coronary Arteries in MSCT Images. In *Proc. of SPIE Medical Imaging* (2003), vol. 5031. 3

[MBHN98] MCCULLOCH A., BASSINGTHWAIGHTE J., HUNTER P., NOBLE D.: Computational Biology of the Heart: From Structure to Function. *Progress in Biophysics and Molecular Biology* (1998). 3

[MKW*02] MEISSNER M., KANUS U., WETEKAM G., HIRCHE J., EHLERT A., STRASSER W., DOGGETT M., FORTHMANN P., PROKSA R.: VIZARDII: A Reconfigurable Interactive Volume Rendering System. In *Proc. of Eurographics/SIGGRAPH Workshop on Graphics Hardware* (2002), pp. 137–146. 6

[MMA02] MONTILLO A., METAXAS D., AXEL L.: Automated Segmentation of the Left and Right Ventricles in 4D Cardiac SPAMM Images. In *Proc. of MICCAI, LNCS 2488* (2002), pp. 620–633. 3

[PMA*99] PARK J., METAXAS D., AXEL L., YUAN Q., BLOM A.: Cascaded MRI-SPAMM for LV Motion Analysis During a Whole Cardiac Cycle. *International Journal of Medical Informatics 55*, 2 (1999), 117–126. 3

[SHN03] SHERBONDY A., HOUSTON M., NAPEL S.: Fast Volume Segmentation With Simultaneous Visualization Using Programmable Graphics Hardware. In *Proc. of IEEE Visualization* (2003), pp. 169–176. 3

[SK99] SRAMEK M., KAUFMAN A.: Alias-free Voxelization of Geometric Objects. *IEEE Transactions on Visualization and Computer Graphics 3*, 5 (1999), 251–266. 7

[SKO*02] S S. S., KOPP A., OHNESORGE B., LOKEGIE H., KÜTTNER A., BAUMBACH A., HERDEG C., CLAUSSEN C., KARSCH K.: Virtual Coronary Angioscopy Using Multislice Computed Tomography. *Heart 87* (2002), 205–209. 3

[SPSP02] SELLE D., PREIM B., SCHENK A., PEITGEN H.: Analysis of Vasculature for Liver Surgery Planning. *IEEE Transactions on Medical Imaging 21*, 11 (2002), 1344–1357. 3

[SSW02] SACHSE F., SEEMANN G., WERNER C.: Modeling of Electro-Mechanics in Left Ventricle. In *Computers in Cardiology* (2002), pp. 705–708. 3

[ST94] SAITO T., TORIWAKI J.: New Algorithms for Euclidean Distance Transformation of an N-Dimensional Digitized Picture with Applications. In *Pattern Recognition* (1994), pp. 1551–1565. 5

[WDGM01] WOLF I., DESIMONE R., GLOMBITZA G., MEINZER H.-P.: EchoAnalyze - A System for Three-Dimensional Echocardiographic Visualization and Quantification. In *Proc. of Computer Assisted Radiology and Surgery* (2001), pp. 902–907. 3

[WMR*01] WAHLE A., MITCHELL S., RAMASWAMY S., CHANDRAN K., SONKA M.: Visualization of Human Coronary Arteries with Quantification Results from 3-D and 4-D Computational Hemodynamics based upon Virtual Endoscopy. In *Proc. of Computer Assisted Radiology and Surgery* (2001), pp. 877–882. 3

[YPW01] YOUNG S., PEKAR V., WEESE J.: Vessel Segmentation for Visualization of MRA with Blood Pool Contrast Agent. In *Proc. of MICCAI, LNCS 2208* (2001), pp. 491–498. 3